Molecular Pharmacology Fast Forward. Published on April 9, 2015 as DOI: 10.1124/mol.114.095398
This article has not been copyedited and formatted. The final version may differ from this version.

Title Page

The Nurr1 activator 1,1-bis(3'-indolyl)-1-(*p*-chlorophenyl)methane blocks inflammatory gene expression in BV-2 microglial cells by inhibiting NF-κB

Briana R. De Miranda, Katriana A. Popichak, Sean L. Hammond, Bryce A. Jorgensen, Aaron T. Phillips, Stephen Safe, and Ronald B. Tjalkens

Center for Environmental Medicine, Department of Environmental and Radiological Health Sciences, Colorado State University, Fort Collins, CO, USA (B.R.D., K.A.P., S.L.H., B.A.J., A.T.P., R.B.T.)

Center for Environmental and Genetic Medicine, Institute of Biosciences and Technology, Texas A&M Health Science Center, Houston, TX, and Department of Veterinary Physiology and Pharmacology, Texas A&M University, College Station, TX, USA (S.S.)

Molecular Pharmacology Fast Forward. Published on April 9, 2015 as DOI: 10.1124/mol.114.095398
This article has not been copyedited and formatted. The final version may differ from this version.

Running Title Page

Running Title:

Novel diindolylmethane analogs inhibit NF-κB in microglia

Corresponding Author:

Ronald B. Tjalkens, Ph.D.

Professor of Toxicology and Neuroscience

Associate Director, Center for Environmental Medicine

Department of Environmental and Radiological Health Sciences

Colorado State University

1680 Campus Delivery

Fort Collins, CO 80523-1680

Tel: 970 491 2825

Fax: 970 491 7569

E-mail: Ron.Tjalkens@colostate.edu

Number of pages, figures, tables, words

Number of text pages:	21
Number of tables:	1
Number of figures:	6
Number of references:	34
Number of words:	5802
Abstract:	235
Introduction:	682
Discussion:	1485

Molecular Pharmacology Fast Forward. Published on April 9, 2015 as DOI: 10.1124/mol.114.095398
This article has not been copyedited and formatted. The final version may differ from this version.

Non-standard abbreviations: [DIM, diindolylmethane; C-DIM, *para*-phenyl substituted diindolylmethane; C-DIM12, 1,1-bis(3'-indolyl)-1-(*p*-chlorophenyl)methane]

Molecular Pharmacology Fast Forward. Published on April 9, 2015 as DOI: 10.1124/mol.114.095398
This article has not been copyedited and formatted. The final version may differ from this version.

Abstract

NR4A family orphan nuclear receptors are an important class of transcription factors for development and homeostasis of dopaminergic neurons that also inhibit expression of inflammatory genes in glial cells. The identification of NR4A2 (Nurr1) as a suppressor of NF-κB-related neuroinflammatory genes in microglia and astrocytes suggests that this receptor could be a target for pharmacological intervention in neurological disease but compounds that promote this activity are lacking. Selected diindolylmethane analogs (C-DIMs) have been shown to activate or inactivate nuclear receptors, including Nurr1, in cancer cells and also suppress astrocyte inflammatory signaling *in vitro*. Based upon these data, we postulated that 1,1-bis(3'-indolyl)-1-(p-chlorophenyl)methane (C-DIM12) suppresses inflammatory signaling in microglia by a Nurr1-dependent mechanism. C-DIM12 inhibited LPS-induced expression of NF-κB-regulated genes in BV-2 microglia including *Nos2*, *Il-6*, and *Ccl2*, and the effects were attenuated by Nurr1-RNA interference. Additionally, C-DIM12 decreased NF-κB activation in NF-κB-GFP reporter cells and enhanced nuclear translocation of Nurr1 primary microglia. Chromatin immunoprecipitation assays indicated that C-DIM12 decreased LPS-induced p65 binding to the *Nos2* promoter and concurrently enhanced binding of Nurr1 to the p65-binding site. Assessment of corepressor recruitment to the p65 binding site of the *Nos2* promoter revealed that C-DIM12 stabilizes the nuclear corepressor complexes CoREST and NCoR2. Collectively, these data identify C-DIM12 as a modulator of Nurr1 activity that results in inhibition of NF-κB-dependent gene expression in glial cells by stabilizing nuclear corepressor proteins that reduces binding of p65 to inflammatory gene promoters.

Molecular Pharmacology Fast Forward. Published on April 9, 2015 as DOI: 10.1124/mol.114.095398
This article has not been copyedited and formatted. The final version may differ from this version.

Introduction

The signaling pathways regulating expression of inflammatory genes in glial cells have been intensely scrutinized for potential therapeutic targets in Parkinson's disease (PD) and related neurodegenerative disorders. Among signaling factors regulating inflammatory gene expression, the nuclear factor-kappa beta (NF-κB) pathway is of considerable interest because it coordinately regulates expression of many pro-inflammatory genes in glia, as well as genes responsible for homeostatic resolution of inflammatory responses (Tansey and Goldberg, 2010; Maguire-Zeiss and Federoff, 2010). Despite increasing attention on the role of NF-κB in glial inflammatory signaling, there are no approved that drugs successfully target this pathway in patients or demonstrate any efficacy in modifying the course of PD or related diseases (Glass et al., 2010; Maguire-Zeiss and Federoff, 2010). Recent studies have demonstrated that cell-specific deletion of NF-κB from microglia or astrocytes is protective in models of inflammatory neurodegeneration (Cho et al., 2008; Brambilla et al., 2005). Results of these knockout studies suggest that selective inhibition of NF-κB could be clinically useful but current pharmacological approaches that globally inhibit NF-κB are likely to have undesirable side effects that outweigh any potential neuroprotective benefits, due to the importance of this pathway in cellular function and homeostasis (Ghosh et al., 1998; Gilmore, 2006).

Within the CNS, there is a high level of regulatory control over inflammatory gene expression in microglia in order to mitigate neuronal injury during responses to stress and infection (Polazzi and Monti, 2010). One possible approach to selectively inhibit NF-κB signaling in microglia without disrupting its homeostatic regulatory functions is to directly target proteins that modulate p50/p65 transcription factors. Such an approach was suggested in studies reporting that transcriptional regulation of NF-κB-inducible genes in astrocytes and microglia is

Molecular Pharmacology Fast Forward. Published on April 9, 2015 as DOI: 10.1124/mol.114.095398
This article has not been copyedited and formatted. The final version may differ from this version.

modulated by NR4A2/Nurr1, a member of the nerve growth factor 1-B family (NGF1-B) of nuclear receptors (Saijo et al., 2009). In addition to transactivation effects, Nurr1 can also negatively regulate gene expression via protein-protein interactions with transcription factors bound to inflammatory promoters via a mechanism termed “transrepression” (Bensinger et al., 2009). Nurr1 is necessary both for development and homeostasis of dopaminergic neurons and has been identified as a genetic mutation involved in familial, late-onset PD (Chu et al., 2006; Saucedo-Cardenas et al., 1998). The discovery that Nurr1 also functions as a transrepressor of NF-κB signaling in glial cells through the active removal of p50/p65 from pro-inflammatory promoters suggests that it could be a possible therapeutic target for limiting glial inflammation (Saijo et al., 2009).

In the present study we evaluated one of a novel series of *para*-phenyl substituted diindolylmethane compounds (C-DIMs) shown to be transcriptional modulators of NR4A family nuclear receptors (Inamoto et al., 2008; Lee et al., 2011; Yoon et al., 2011). Selected C-DIMs, such as *para*-phenyl diindolylmethane (1,1-bis(3′-indolyl)-1-(p-chlorophenyl) methane; C-DIM12), activates Nurr1 in urothelial carcinoma cells (Inamoto et al., 2008) and in pancreatic cells (Li et al., 2012). We previously demonstrated that another C-DIM, 1,1-bis(3′-indolyl)-1-(p-methoxyphenyl) methane (C-DIM4), suppressed NF-κB activation and inhibited inflammatory gene expression in primary astrocytes, leading to decrease of expressed *Nos2* and *Tnfα* (Carbone et al., 2008). Based on these observations, C-DIM12 was selected for *in vivo* efficacy studies in a mouse model of PD using subacute dosing with 1-methyl-4-phenyl-1,2,3,6-tetrahydropyridine (MPTP) in combination with probenecid (MPTPp) to induce progressive loss of dopaminergic neurons in the substantia nigra (SN; De Miranda et al., 2013). When delivered orally after one

Molecular Pharmacology Fast Forward. Published on April 9, 2015 as DOI: 10.1124/mol.114.095398
This article has not been copyedited and formatted. The final version may differ from this version.

week of dosing with MPTPp, C-DIM12 protected against loss of dopamine neurons in the substantia nigra (SN), as well as dopamine terminals in the striatum (ST).

It remains unclear what whether C-DIM12 can directly inhibit inflammatory gene transcription in microglial cells, despite the evidence that it is able to reduce dopamine neuron loss *in vivo*. We therefore postulated that C-DIM12 inhibits inflammatory signaling in BV-2 microglia cells by enhancing Nurr1-dependent transrepression of NF-κB at proinflammatory gene promoters. We present data here that C-DIM12 is able to suppress pro-inflammatory gene transcription in BV-2 microglia after stimulation with LPS. Additionally, we investigated whether the transcriptional inhibitory activity of C-DIM12 requires expression of Nurr1 and how modulation of Nurr1 by C-DIM12 affects the activity of nuclear corepressor proteins at p65 DNA binding sites.

Molecular Pharmacology Fast Forward. Published on April 9, 2015 as DOI: 10.1124/mol.114.095398
This article has not been copyedited and formatted. The final version may differ from this version.

Materials and Methods

Reagents. C-DIM compounds were synthesized by Dr. Stephen Safe and characterized as described in (Qin et al., 2004). Lipopolysaccharide from Escherichia coli 0111:b4 (LPS), NF-κB inhibitor Bay-11-7082 (Bay-11) and all general chemical reagents were purchased from Sigma-Aldrich (St. Louis, MO) unless stated elsewhere. Tumor necrosis factor alpha (TNFα) was purchased from R & D Systems, Inc. (Minneapolis, MN). Antibodies used in immunofluorescence experiments were purchased from Cell Signaling Technology (p65; Danvers, MA), Santa Cruz Biotechnology, Inc. (Nurr1; Dallas, TX) and BD Biosciences (CD11b; San Jose, CA).

Cell Culture Experiments. BV-2 microglia were obtained as a generous gift from Dr. Alan Schenkel, Professor of Microbiology, Immunology and Pathology, Colorado State University, Fort Collins, CO. BV-2 cells were maintained at or below passage 10, cultured in DMEM (supplemented with L-glutamine; Gibco) containing 10% FBS (heat-inactivated fetal bovine serum, Atlanta Biologicals) and a cocktail of 0.001 mg/ml penicillin, 0.002 mg/ml streptomycin, 0.001 mg/ml neomycin; (1x PSN; Hyclone). BV-2 cells were grown until 60-70% confluent before treatments. Primary mixed glia were obtained through cortical isolations from C57/Bl6 mouse pups (P0, unknown genders). Mixed glial cultures were maintained in MEM (supplemented with L-glutamine; Hyclone), 10% FBS, and 1x PSN as described above. Primary glial cultures were grown until 80% confluent before treatments. Glial purification by our lab was preformed as described in Carbone et al., 2008. All cell cultures were maintained at 37□ and 5% CO_2. All procedures involving animals were approved by the Colorado State University Institutional Animal Care and Use Committee (IACUC), and were conducted in accordance with current NIH guidelines.

Molecular Pharmacology Fast Forward. Published on April 9, 2015 as DOI: 10.1124/mol.114.095398
This article has not been copyedited and formatted. The final version may differ from this version.

Gene Knockdown Assays. RNA interference (siRNA) sequences were obtained through Integrated DNA Technologies, Inc. (IDTDNA; Coralville, IA) and Ambion (Life Technologies, Grand Island, NY). Nurr1 RNAi duplexes were designed against splice common variants of the target gene, and were validated using a dose-response assay with increasing concentrations of the suspended oligo (150-450 ng/μl) using a standard scrambled dsiRNA as control. RNAi oligos were transfected using *Trans*IT-X2 delivery system (Mirus Bio LLC, Madison, WI) 24 hours prior to C-DIM12 or LPS treatment. Separate siRNA systems were used to ensure specific knockdown of Nurr1 mRNA, while limiting off-target effects on other nuclear receptor family members (Nur77, Nor1) or corepressor proteins. Nurr1 siRNA sense sequence; (5'-> 3') GCAUCGCAGUUGCUUGACAtt, antisense, UGUCAAGCAACUGCGAUGCgt (Ambion *Silencer* Select siRNA; denoted RNAi-2). DsiRNA duplex sequences; (5'-> 3') CUAGGUUGAAGAUGUUAUAGGCACT; AGUGCCUAUAACAUCUUCAACCUAGAA (IDT dsiRNA; denoted RNAi-1).

Gene Expression Assays. Quantitative reverse transcriptase PCR (qRT-PCR) primers were synthesized by IDT Integrated DNA Technologies (Supplemental Table 1). BV-2 cells were pre-treated with 10 μM C-DIM12 (0.1 μM, 1.0 μM, or 10 μM in dose-response assays) for one hour in serum and antibiotic free OptiMEM (Gibco) prior to treatment with 1 μg/ml lipopolysaccharide (LPS, Sigma-Aldrich, St. Louis, MO). RNA was isolated using an RNeasy Mini kit (Qiagen, Valencia, CA) and purity and concentration was determined using a NanoVue Spectrophotometer (GE Healthcare). After purification, 1 μg of RNA was used as a template for reverse transcriptase (RT) reactions using iScript (BioRad, Hercules, CA). cDNA produced from this reaction was measured for gene expression levels of proinflammatory genes using an Eco Real-Time PCR System (Illumina, Inc. San Diego, CA). Relative changes from control

Molecular Pharmacology Fast Forward. Published on April 9, 2015 as DOI: 10.1124/mol.114.095398
This article has not been copyedited and formatted. The final version may differ from this version.

conditions (expressed as fold change) in gene expression were calculated using the $2^{-\Delta\Delta C}{}_T$ method and normalized using the β-actin and HPRT housekeeping genes (Livak and Schmittgen, 2001). Samples were run in duplicate, and biological replicates were repeated from a minimum of three separate experiments.

NF-κB Reporter Assays. The NF-κB-293T-GFP-Luc reporter cell line was purchased from System Biosciences (Mountain View, CA). For GFP/DAPI expression assays, cells were grown in DMEM (Life Technologies, Grand Island, NY) supplemented with 10% FBS, 1X PSN (as described above), on 96 well black-walled plates (Thermo Scientific, Waltham, MA). Cells were plated 24 hours prior to treatment with 30 ng/ml TNFα in the presence or absence of 100 μM of C-DIM12 or 50 μM of Bay-11-7082 (Bay-11, positive control) for 24 hours, or at specific time/dosage as described in figure legends. Reporter cells were then washed with 1X PBS and stained with Hoechst 33342 (Molecular Probes) in Fluorobrite DMEM (Life Technologies) incubated at 37° C, 5% CO2 for 5 minutes and washed again with 1X PBS. Media was replaced with fresh Fluorobrite DMEM before reading plate at 488/519 nm for GFP fluorescent expression and 345/478 nm for DAPI fluorescent expression on Cytation3 Cell Imaging Multi-Mode Reader (BioTek Instruments, Winooski, Vermont). GFP expression intensity values were divided over DAPI expression intensity values for quantitative analysis. TNFα concentrations were based on a dose response assay (0-100 ng/ml; Supplemental Figure 1) for optimal induction of NF-κB-GFP expression.

Chromatin Immunoprecipitations (ChIP). BV-2 cells were grown to confluence in 10-cm tissue culture plates (approximately 2 x 10^7 cells) and treated for the indicated time with LPS (1 μg/ml), with or without C-DIM12 (10 μM) or a DMSO vehicle control before cross-linking with 1% formaldehyde (Thermo Scientific) for 10 min. The remaining steps were adapted from the

Molecular Pharmacology Fast Forward. Published on April 9, 2015 as DOI: 10.1124/mol.114.095398
This article has not been copyedited and formatted. The final version may differ from this version.

Chromatrap ChIP protocol, which accompanies the Chromatrap Pro-A Premium ChIP Kit (Chromatrap, Wrexham, UK). DNA was sheared into approximately 500 base pair fragments before removing 10% (200 ng) for input controls, and 2 μg of chromatin was loaded into the immunoprecipitation (IP) reaction with 2 μg precipitating antibody (as suggested by Chromatrap), Anti-CoREST (32631), anti-NCOR2 (5802), and anti-HDAC3 (7030) from Abcam (Cambridge, UK); anti-Nurr1 (N-20; 991), and anti-p65 (372) from Santa Cruz Biotechnology (Dallas, TX). Immunopurified DNA was isolated via the QIAquick™ PCR Purification Kit (28104; suggested by Chromatrap). A 149 bp region of the *Nos2* promoter proximal to the NF-κB site of transcription was amplified via quantitative-PCR and performed with SYBR-Green Supermix (Bio-Rad, Hercules, CA) and analyzed using the percent input method according to Life Technologies™.

Immunoblotting. BV-2 cells were lysed using RIPA buffer with protease inhibitors. Protein was quantified using a BCA protein assay (Thermo Scientific Pierce, Rockford Il) and equal protein (20 μg) was loaded in a polyacrylamide 12% gel with 4% stacking gradient. Protein quantitation was imaged using a Biorad ChemiDoc XRS System and compared to β-actin control using ImageJ analysis software (Schneider et al., 2012). ChIP-grade antibodies, as reported above, were used at a 1:1000 concentration for western blot analysis; phospho-p65 antibody serine 486 (Ab 3039; Cell Signaling Technology).

Immunofluorescence Microscopy in BV-2 Cells. BV-2 microglia were plated on cover glass coated with FBS and pre-treated for one hour with 10 μM of C-DIM12 followed by 1 μg/ml LPS. After 30 minutes the cells were rinsed with PBS buffer and then paraformaldehyde fixed for 15 min at 4□. Cells were blocked using bovine serum albumin (BSA; Sigma-Aldrich, St. Louis, MO) for one hour until incubation with primary antibodies overnight at 4□. Secondary

Molecular Pharmacology Fast Forward. Published on April 9, 2015 as DOI: 10.1124/mol.114.095398
This article has not been copyedited and formatted. The final version may differ from this version.

antibody incubation was at room temperature for 3 hours; Alexa Fluor 555, Alexa Fluor 647 (Life Technologies), DAPI counterstain (Vector Labs, Burlingame, CA). Slides were imaged using a Zeiss Axiovert 200M inverted fluorescence microscope equipped with a Hammamatsu ORCA-ER-cooled charge-coupled device camera (Hammamatsu Photonics, Hamamatsu City, Japan) using Slidebook software (version 5.5; Intelligent Imaging Innovations, Denver, CO). Quantification of nuclear protein was determined by measuring the fluorescence intensity of p65 or Nurr1 within the boundary of the nucleus of each cell, defined by DAPI counterstain, and segmented using Slidebook 5.0 software function for fluorescence intensity minus background (F/F_o).

Confocal Microscopy in Primary Microglia. Primary mouse microglia were seeded on 12 mm round microscopic coverglass slides coated with fetal bovine serum and allowed attach and grow for 48 hrs prior to experimentation. Cells were treated for 1 hour with saline, 1 μg/ml LPS, or 1 μg/ml LPS + 10 μM C-DIM12, fixed in ice-cold methanol and probed with anti-CD11b-FITC (1:250) and anti-Nurr1 (1:500). Nurr1 was visualized with an AlexaFluor-555 conjugated secondary antibody. Microglia were imaged on an Olympus Fluoview 1000 laser-scanning confocal microscope using a 100X Plan Apochromat oil immersion objective. Each field of view was imaged as a z-stack with a (8-10 planes, 1 μm step size) to ensure images included all planes associated with the cells being imaged. The resulting z-stacks were transformed into a single maxium projection image over the z-plane using the Stack Focuser plug-in within Fiji (NIH open-source image processing software).

Statistical Analysis. Statistical analyses were performed using Prism (version 6.0; Graph Pad Software, San Diego, CA). Data are presented as mean ± SEM. Experimental group analyses

Molecular Pharmacology Fast Forward. Published on April 9, 2015 as DOI: 10.1124/mol.114.095398
This article has not been copyedited and formatted. The final version may differ from this version.

were preformed using a one-way ANOVA with a Tukey post hoc test. Statistical significance was considered at $p< 0.05$ (*), $p< 0.001$ (**), $p< 0.001$(***), $p< 0.0001$ (****).

Results

Structure-activity of C-DIMs in suppression of pro-inflammatory genes

Initial analysis of a series of C-DIM analogs (C-DIM1 through C-DIM14) was performed to determine their effect on inflammatory gene expression in primary mixed cultures of astrocytes and microglia (Li et al., 2012). In order to assess the efficacy and structure-activity relationships of C-DIM compounds on expression of representative NF-κB-regulated neuroinflammatory genes, primary mixed glia were treated with 1 μg/ml LPS and either 1 μM or 10 μM of each C-DIM compound (Table 1). Compared to LPS treatment alone, several of the C-DIM compounds (C-DIMs 1, 3, 5, 7, 8, 10, 11, 12, 13) significantly decreased *Nos2* and *IL-1β* expression at a concentration of 10 μM. The substituted -*R* position of the *para*-phenyl group appeared to change the anti-inflammatory activity of specific C-DIMs, consistent with a structure-activity relationship (SAR) indicating that C-DIMs with smaller, more polar *para* substituents on the phenyl group are even more potent as suppressors of inflammatory gene expression in primary mixed glial cells. This SAR study showed that C-DIM5, and C-DIM12, which contain *para*-methoxy- (C-DIM5) and *para*-chloro-phenyl substituents (C-DIM12; NR4A2/Nurr1 activity), suppressed *Nos2* and *Il-1β*, whereas phenyl-substituted C-DIM9 did not decrease LPS-induced expression of these inflammatory genes (Figure 1A-B). Based on these results and on previous pharmacokinetic and efficacy screening of C-DIMs in mice (De Miranda

Molecular Pharmacology Fast Forward. Published on April 9, 2015 as DOI: 10.1124/mol.114.095398
This article has not been copyedited and formatted. The final version may differ from this version.

et al., 2013), we selected C-DIM12 (Figure 1C) for further *in vitro* analysis of its mechanism of inhibition of inflammatory cytokine expression in microglia.

C-DIM12 decreases inflammatory gene expression in BV-2 microglia

Cytokine expression in glia is well documented both *in vivo* and *in vitro* following stimulation of microglial TLR receptors and subsequent IKK-dependent activation of NF-κB (Saijo et al., 2013). BV-2 microglia were challenged with 1 μg/ml LPS and assayed for the time course of expression of the NF-κB-regulated genes *Nos2, Tnfα, Il-6, Il-1β Ccl5*, and *Ccl2* over a period of 24 hours (Figure 1D-I). All genes assayed were maximally induced at 24 hours after LPS treatment with the exception of *Il-1β*, which peaked after 2 hours followed by a decline in expression that remained above control levels. We next examined the potency of C-DIM12 in suppressing the expression of selected neuroinflammatory genes (Figure 2A-F) by treating BV-2 cells with LPS (10 μg/ml) for 24 hours in the presence of increasing concentrations of C-DIM12 (0, 0.1, 1, or 10 μM). Inflammatory gene expression of *Nos2*, *Il-6*, and *Ccl5* were significantly decreased over LPS and vehicle control (DMSO) expression levels with 1 μM of C-DIM12, whereas *Tnfα* and *Ccl2* were significantly suppressed with 10 μM C-DIM12. A trend toward suppression of *Il-1β* is evident, and a higher concentration of C-DIM12 may be required to elicit a significantly decreased response (Figure 2D).

C-DIM12 decreases expression of NF-κB-EGFP expression in HEK 293 cells reporter cells

Molecular Pharmacology Fast Forward. Published on April 9, 2015 as DOI: 10.1124/mol.114.095398
This article has not been copyedited and formatted. The final version may differ from this version.

In order to further examine the effect C-DIM12 on NF-κB transcriptional activity, we exposed NF-κB-GFP HEK cells (NF-κB/293/GFP-Luc Transcriptional Reporter Cells; System Biosciences, Mountain View, CA) to TNFα in the presence of C-DIM12 (Figure 2G-J). These cells stably express an NF-κB reporter construct consisting of high affinity p65 binding sites driving co-expression of GFP and luciferase in response to stimulation with TNFα (Figure 2G). Exposing NF-κB-GFP HEK cells to increasing concentrations of TNFα (1-100 ng/ml) for 24 hours resulted in a dose-dependent increase in total GFP fluorescence per cell (Figure 2H). Co-treatment with C-DIM12 (100 μM) significantly reduced TNFα (30 ng/ml)-induced NF-κB-GFP expression, comparable to that observed for BAY-11-7082 (BAY11, 50 μM), a positive control for inhibition of NF-κB that blocks IκB kinase (IKK) activity (Krishnan et al., 2013). C-DIM12 (100 μM) and BAY11 (50 μM) were equally efficient at blocking NF-κB-GFP expression in the NF-κB-GFP HEK cells after TNFα treatment, displaying statistically significant reduction in total GFP fluorescence per cell (Figure 2I). The time course for C-DIM12-dependent suppression of TNFα-induced NF-κB-GFP was examined in Figure 2J, where no detectable increase in NF-κB-GFP fluorescence was observed up to 24 hours in cells exposed to 30 ng/ml of TNFα in the presence of 100 μM C-DIM12 ($p < 0.0001$ compared to TNFα plus DMSO vehicle control).

Nurr1 is required for suppression of inflammatory genes by C-DIM12

Previous data indicated that lentiviral-mediated RNAi knockdown of Nurr1 increases both basal and inducible levels of inflammatory cytokines in BV-2 microglial cells and enhances loss of dopamine neurons in the substantia nigra (SN) after LPS treatment (Saijo et al., 2009). We therefore used RNAi to examine the capacity of C-DIM12 to function as a pharmacologic

Molecular Pharmacology Fast Forward. Published on April 9, 2015 as DOI: 10.1124/mol.114.095398
This article has not been copyedited and formatted. The final version may differ from this version.

modulator of Nurr1 though its effects on transrepression of NF-κB-regulated inflammatory genes. The data in Figure 3A indicated that treatment of BV-2 microglia with two different sequences of small interfering RNA against Nurr1 (RNAi-1 or RNAi-2) resulted in significant knockdown of Nurr1 mRNA expression. To address whether knockdown of Nurr1 affected other NR4A family members (NR4A1/*Nur77, NR4A3/Nor1*) mRNA expression was assayed following Nurr1 RNAi treatment, which did not result in significantly altered gene expression, though *Nur77* mRNA shows a trend toward decrease compared to control in RNAi-2-treated cells, and Nor1 shows a trend toward increasing in RNA-1-treated cells, respectively (Figure 3B-C). Expression of corepressor proteins involved in Nurr-1 mediated transrepression (*NCoR2, CoREST,* and *HDAC3*) were unaffected by RNAi interference, (Figure 3D). Nurr1 RNAi enhanced expression of *Nos2* after 24 hours of stimulation with LPS (Figure 3E). This same trend was observed with *Tnfα,* though not statistically significant (Figure 3F). Following RNAi knockdown of Nurr1, BV-2 cells were also treated with LPS in both the presence and absence of C-DIM12 (10 μM) for 24 hours and then assayed for expression of representative NF-κB-regulated inflammatory genes, *Nos2*, *Tnfα*, *Il-1β* and *Il-6* (Figure 3G-J). In treatment groups receiving Nurr1 RNAi, C-DIM12 no longer suppressed LPS-induced expression *Nos2*, *Tnfα, Il-1β,* and *Il-6* (Figure 3G-J). These data indicate that C-DIM12 requires expression of Nurr1 in order to fully suppress proinflammatory gene expression in BV-2 cells stimulated by LPS.

NF-κB-p65 translocation is not inhibited by C-DIM12

Binding of LPS to TLR4 receptors in microglia activates NF-κB through IKK-dependent phosphorylation and degradation of IκBα, leading to translocation of p50/p65 heterodimers into

Molecular Pharmacology Fast Forward. Published on April 9, 2015 as DOI: 10.1124/mol.114.095398
This article has not been copyedited and formatted. The final version may differ from this version.

the nucleus where they activate inflammatory gene promoters at *cis*-acting promoter elements (He et al., 2002; Saijo et al., 2013). To determine whether C-DIM12 inhibited inflammatory gene expression by preventing translocation of p65 to the nucleus, we treated BV-2 microglial cells with 1 μg/ml LPS and measured the nuclear translocation of p65 using immunofluorescence. After 30 minutes, p65 levels in the nucleus of BV-2 cells were markedly increased over saline control (Figure 4A), indicated by the disappearance of nuclear voids evident prior to LPS treatment. C-DIM12 did not inhibit nuclear translocation of p65 in BV-2 microglia treated with 1 μg/ml LPS, but rather enhanced nuclear levels of p65 (Figure 4B).

It was recently reported that GSK3β is required for binding of Nurr1 to p65 at inflammatory gene promoters (Saijo et al., 2009). Phosphorylation of p65 at serine 486 provides the docking site necessary to recruit Nurr1 to p65 and thereby block the removal of transcriptional inhibitory protein complexes at inflammatory gene promoters (Saijo et al., 2009). Protein expression of phosphorylated p65 after treatment with SB216763 (SB21), an inhibitor of GSK3β, indicated that LPS-induced p65 phosphorylation of serine 486 was decreased following GSK3β inhibition (Figure 4C-D). C-DIM12 treatment did not significantly alter the amount of phosphorylated p65; though a trend of decreased phosphorylation is visible, which correlates to global NF-κB suppression that was observed following C-DIM12 treatment. To determine whether C-DIM12 requires GSK3β to block LPS-induced expression of neuroinflammatory genes, we treated BV-2 cells with SB21 and challenged them with 10 μg/ml LPS for 24 hours with and without the co-treatment of C-DIM12. When GSK3β was inhibited, expression of *Nos2* and *Tnfα* were both significantly induced in BV-2 cells, both in the presence and absence of C-DIM12 (Figure 4E-F).

Molecular Pharmacology Fast Forward. Published on April 9, 2015 as DOI: 10.1124/mol.114.095398
This article has not been copyedited and formatted. The final version may differ from this version.

C-DIM12 modulates cellular localization of Nurr1

Because suppression of LPS-induced expression of inflammatory genes by C-DIM12 required functional levels of Nurr1, we sought to determine whether C-DIM12 altered the expression or subcellular localization of Nurr1 in microglia. Highly enriched cultures of primary mouse microglia were treated with LPS (10 ng/ml) or with LPS + C-DIM12 (10 μM) and Nurr1 protein expression and subcellular localization was examined by confocal microscopy (Figure 5A-C; Nurr1 - red, CD11b - green, DAPI - blue). Nurr1 expression was visibly increased over saline in microglia treated with LPS and pronounced nuclear translocation of Nurr1 was evident with colocalization of Nurr1 and DAPI in merged images. Quantitation of fluorescence intensity of Nurr1 protein colocalizing with the cytoplasm or the nucleus resulted in a significant increase of nuclear Nurr1 in microglia treated with LPS + C-DIM12 (Figure 5D-E). Additionally, LPS and LPS + C-DIM12 treatments significantly increased *Nurr1* mRNA after 24 hours (Figure 5C). Despite the observation that Nurr1 expression and nuclear localization were equivalent between LPS and LPS + C-DIM12 groups, LPS-induced expression of *Il-6* and *Nos2* was significantly suppressed only in the LPS + C-DIM12 treatment groups (Figure 5 G-H), indicating that C-DIM12 may not further increase Nurr1 above LPS-induced levels in BV-2 cells but may activate or enhance Nurr1-dependent function in microglia.

Nurr1 transcriptional repression is enhanced by C-DIM12

Recruitment of Nurr1 monomers to p65 involves several proteins with kinase action (GSK3β, NLK), as well as proteins that modify Nurr1 in order to recruit corepressors such as histone deacetylases (HDAC2/3), nuclear receptor co-repressor 2 (NCoR2) and the CoREST

Molecular Pharmacology Fast Forward. Published on April 9, 2015 as DOI: 10.1124/mol.114.095398
This article has not been copyedited and formatted. The final version may differ from this version.

complex (Saijo et al., 2009). We performed chromatin immunoprecipitation (ChIP) assays to determine the capacity of C-DIM12 to modulate protein-DNA interactions at NF-κB binding sites in the Nos2 promoter (Figure 6), postulating that C-DIM12-dependent activation of Nurr1 would stabilize corepressor protein complexes at NF-κB *cis*-acting promoter elements. Time course data indicate that in BV-2 microglia treated with 10 μg/ml LPS, p65 binding to the Nos2 promoter increased and remained elevated for up to 24 hours (Figure 6A), whereas co-treatment with C-DIM12 (10 μM) significantly reduced the amount of p65 binding ($p< 0.001$ relative to LPS + C-DIM12). Simultaneously, Nurr1 was strongly recruited to the p65 binding site by 24 hours in cells treated with LPS + C-DIM12 (Figure 6B; $p< 0.0001$, relative to LPS + DMSO vehicle control). Overall, BV-2 cells treated with LPS + C-DIM12 had a significantly lower amount of p65 bound to the Nos2 promoter throughout the 24 hour time course.

DNA binding and expression of the corepressor proteins NCoR2 and CoREST were also examined under these conditions. In cells treated with LPS + C-DIM12, cyclic increases in NCoR2 bound to the Nos2 promoter occurred 2 and 8 hours after LPS treatment (Figure 6C; $p< 0.001$ and $p< 0.0001$ compound to LPS + DMSO vehicle control). In contrast, CoREST binding to the Nos2 promoter increased three-fold by 2 hours in both the LPS and LPS + C-DIM12 groups, but remained elevated at 24 hours in the LPS + C-DIM12 group (Figure 6D; $p< 0.01$ compared to LPS + DMSO vehicle control). In summary, cells treated with C-DIM12 had sustained levels of both Nurr1 and CoREST bound to the Nos2 promoter 24 hours after exposure to LPS in the presence of C-DIM12, which correlated with decreased binding of p65.

Representative protein expression of total p65 shows an apparent decrease from LPS treatment with the addition of C-DIM12 (Figure 6E), however as consistent with mRNA expression, Nurr1 protein levels are not significantly altered by C-DIM12 treatment (Figure 6F).

Molecular Pharmacology Fast Forward. Published on April 9, 2015 as DOI: 10.1124/mol.114.095398
This article has not been copyedited and formatted. The final version may differ from this version.

Protein expression of NCoR2, HDAC3 and Co-REST were determined in BV-2 cells over 24 hour exposure to LPS and LPS + C-DIM12 (Figure 6G). Immunoblot data from these experiments indicates that NCoR2, CoREST and HDAC3 protein levels decreased slightly after LPS treatment (4 hr) however, no significant differences were detected at the level of total protein expression (Figure 6 H-J). A schematic depicting the proposed activation of Nurr1 by C-DIM12 is illustrated in Figure 6K, represented as an adaptation from the mechanism described by Saijo et al., 2009. The hypothesized mechanism includes the enhanced binding of Nurr1 to the NF-κB response element region of the promoter, and the recruitment of corepressor complexes responsible for the decrease in p65 bound to the Nos2 promoter in microglial cells.

Molecular Pharmacology Fast Forward. Published on April 9, 2015 as DOI: 10.1124/mol.114.095398
This article has not been copyedited and formatted. The final version may differ from this version.

Discussion

The nuclear receptor NR4A2/Nurr1 is described as a potential therapeutic target for mitigating the damaging effects of glial activation but compounds that selectively modulate this receptor to inhibit NF-κB-regulated neuroinflammatory genes have not been reported (Bensinger et al., 2009; Nolan et al., 2013). C-DIM12 was selected for examination in this study following several lines of evidence for its use as a potential neuroprotective compound. C-DIM12 displays the ability to suppress inflammatory gene expression in astrocytes *in vitro* (Table 1) and it has significant distribution to the brain following oral dosing (De Miranda et al., 2013). In an *in vivo* MPTPp mouse model of PD, post-lesion treatment with C-DIM12 attenuated dopamine neuron loss and reduced glial activation and cytokine induction with greater significance than other C-DIM compounds (De Miranda et al., 2014). The data presented here indicate that C-DIM12 suppresses NF-κB-induced gene expression in microglia through a mechanism involving transcriptional repression via Nurr1 (Saijo et al., 2009). Structure-activity studies indicated that C-DIM12 and related halogenated C-DIM structures had more potent anti-inflammatory action in primary mouse mixed glia than several other C-DIM analogs with bulkier aliphatic or aromatic substituents (Figure 1; Table 1). The structure-dependent binding of some C-DIMs to the ligand-binding domain of NR4A1 has been reported (Lee et al., 2014), and these compounds can either activate or inactivate NR4A1 and NR4A2-dependent transactivation in a structure-specific manner (Dae Cho et al., 2010; Li et al., 2012; Yoon et al., 2011). Through this mechanism, these studies indicated that C-DIM12 inhibits growth of urothelial carcinoma cells (KU7, 253J cell lines) and also decreased tumor growth *in vivo* (Inamoto et al., 2008). The anticancer properties of C-DIM12 were Nurr1-dependent, (Inamoto et al., 2008), however the effects on of this compound on Nurr1 in normal cells have been less well studied and are likely

Molecular Pharmacology Fast Forward. Published on April 9, 2015 as DOI: 10.1124/mol.114.095398
This article has not been copyedited and formatted. The final version may differ from this version.

to involve distinct protein complexes of transcription activators and repressors, and other nuclear cofactors.

Dose-dependent inhibition of inflammatory gene expression in BV-2 microglia indicated that C-DIM12 blocks expression of NF-κB-regulated inflammatory cytokines and chemokines (Figure 2). In addition, C-DIM12 suppressed NF-κB activation in NF-κB-GFP HEK reporter cells stimulated with TNFα (Figure 2I-J) but did not prevent the nuclear translocation of p65 in BV-2 cells exposed to LPS (Figure 4A). These findings indicate that C-DIM12 acts downstream of NF-κB-p50/65 translocation and therefore likely prevents transcriptional activation of NF-κB-regulated genes by a direct effect on the transcriptional activity of nuclear proteins, rather than on prevention of upstream NF-κB activating kinases. The observed increase in nuclear p65 following LPS + C-DIM12 treatment may be indicative of an increased amount of Nurr1 bound to p65, causing an accumulation in the nucleus. Knockdown of Nurr1 by RNAi-1 markedly decreased the ability of C-DIM12 to suppress mRNA levels for multiple inflammatory genes (Figure 3G-J), indicating that the transrepressive activity C-DIM12 likely requires Nurr1. Moreover, knockdown of Nurr1 had no effect on the effect on the expression of corepressor proteins NCoR2, CoREST or HDAC3, supporting the conclusion that C-DIM12 directly modulates Nurr1 and not its downstream effector proteins. It cannot be completely ruled out that a change in expression of Nur77 or Nor1 (Figure 3B,C) may contribute to the alteration of inflammatory gene expression that was observed following Nurr1 RNAi, however such gene interactions are poorly understood in glia and warrant a comprehensive study of their own.

Nurr1-mediated transrepression of *Nos2* in BV-2 microglia involves the recruitment of the CoREST corepressor complex to remove p65 (Saijo et al., 2009). The transrepressive activity of Nurr1 towards NF-κB requires phosphorylation of p65 at serine-468 by GSK3β, and

Molecular Pharmacology Fast Forward. Published on April 9, 2015 as DOI: 10.1124/mol.114.095398
This article has not been copyedited and formatted. The final version may differ from this version.

inhibition of GSK3β significantly increases the transcription of NF-κB-regulated genes such as Tnfα and Nos2 (Buss et al., 2002; Saijo et al., 2009). We noted a similar effect with C-DIM12 (Figure 4), where the GSK3β inhibitor, SB21, reduced the capacity of C-DIM12 to suppress LPS-induced expression of *Nos2* and *Tnfa*. This suggests that C-DIM12-mediated repression also requires phosphorylation of p65 for recruitment of Nurr1 and inhibition of p65 transcriptional activation. The studies in Figure 3 indicated that C-DIM12 did not suppress LPS-induced expression of *Il-1β* to the same extent as the other cytokines assayed, likely because expression of *Il-1β* in microglia is highly regulated by MAPK pathways in addition to NF-κB, which appears to support the specificity of C-DIM12 for suppression of NF-κB-regulated proteins (Kim et al., 2004). However, RNAi studies (Figure 3I) indicated that knockdown of Nurr1 expression significantly attenuated the inhibitory effects of C-DIM12 on LPS-induced expression of *Il-1β*, supporting the importance of NF-κB/Nurr1 interactions in regulating this pathway. While cross-talk between inflammatory cascade proteins is known to occur upon stimulation of toll-like receptors on the surface of cells, it is likely that MAPK proteins are able to separately upregulate *Il-1β* expression independently of NF-κB. Therefore, suppression of p65-mediated inflammatory gene transcription likely results in only partial suppression of *Il-1β*.

The NR4A family of nuclear receptors are described as immediate-early response genes involved in cellular maintenance and development, as well as in regulating inflammation (Zhao and Bruemmer, 2010). Although Nurr1 is primarily located in the nucleus in neurons and cancer cells (Debernard and Mathisen, 2012; García-Yagüe et al., 2013; Li et al., 2012), our data in primary microglia suggest that Nurr1 is dynamically regulated in glial cells and its subcellular localization changes following inflammatory stimulation with LPS (Figure 5). This is supported by previous studies reporting that stimulation of TLR4 with LPS causes nuclear import of Nurr1,

Molecular Pharmacology Fast Forward. Published on April 9, 2015 as DOI: 10.1124/mol.114.095398
This article has not been copyedited and formatted. The final version may differ from this version.

although the mechanisms regulating this effect are not well understood (Fan et al., 2009). Additionally, the cellular distribution of Nurr1 appears to vary between cell types. In SH-SY5Y and MN9D neuronal cell lines, changes in the subcellular localization of Nurr1 occurred within 1 hour of sodium aresenite-induced oxidative stress that caused exposure of a nuclear export signal (NES; García-Yagüe et al., 2013), thereby decreasing its transcriptional activity. Similarly, the intracellular location of NR4A1/Nur77 in cancer cells is variable; for example, treatment with apoptosis-inducing agents induces nuclear export of Nur77 where it forms a complex with Bcl-2 on mitochondria (Zhang et al., 2009), whereas the C-DIMs that bind the receptor activate or inactivate nuclear Nur77 (Lee et al., 2014). In non-neuronal cells, nuclear import signals (NIS) on Nurr1 may be alternatively uncovered for import into the nucleus for feedback inhibitory control over inflammatory proteins, although the mechanism is not well established (García-Yagüe et al., 2013). Here, we report that the translocation of Nurr1 from the cytosol to the nucleus in primary microglia treated with LPS occurred in both the presence and absence of C-DIM12 (Figure 5A-B). Inflammatory gene expression however, was only blocked in the presence of C-DIM12, despite increases in Nurr1 mRNA in both groups, indicating that C-DIM12 likely stimulates the anti-inflammatory activity of Nurr1 by direct action on nuclear proteins.

The use of ChIP assays to examine the effects of C-DIM12 on LPS-induced protein-DNA interactions (Figure 6) revealed that initial increases in p65 binding to the *Nos2* promoter were maintained up to 24 hours, consistent with the time course for suppression of inflammatory gene expression (Figures 2A, 6A). C-DIM12 decreased p65 interaction at the *Nos2* promoter, with greatest reduction seen at 24 hours. The interaction of Nurr1 with the *Nos2* promoter was also increased in cells treated with C-DIM12, with a marked increase in recruitment of Nurr1 to the

Molecular Pharmacology Fast Forward. Published on April 9, 2015 as DOI: 10.1124/mol.114.095398
This article has not been copyedited and formatted. The final version may differ from this version.

promoter regions encompassing the p65 binding site at 24 hours (Figure 6B). In addition, the amount of CoREST and NCoR2 bound to the *Nos2* promoter was increased over LPS (24 hr) in cells treated with C-DIM12, a mechanism that corresponds with the reduction of inflammatory gene expression in BV-2 microglia (Figure 2G, 6C,D). Total protein levels of Nurr1, NCoR2, CoREST, and HDAC3 (Figure 6E-G) are additional evidence that C-DIM12 action does not produce sizeable increases in corepressor proteins, but instead may enhance Nurr1-mediated recruitment of corepressors that mediate transrepression of inflammatory genes in microglia. Consistent with these findings, there were no significant changes in the expression of either p65 or Nurr1 between LPS and LPS + C-DIM12 treatment groups (Figure 6 E,F). A theoretical model for the anti-inflammatory action of C-DIM12 is illustrated in Figure 6H, where *Nos2* promoter transcription activated by NF-κB-p50/p65 is reduced by corepressor complex proteins (HDAC, NCoR2, and CoREST) that are recruited to the *Nos2* promoter by Nurr1. Pharmacologic modulation of Nurr1 by C-DIM12 increases the nuclear receptor interactions with corepressor proteins, preventing binding of the RNA polymerase complex and leading to eventual removal p65 from the *Nos2* promoter, thereby reducing inflammatory gene transcription.

The discovery of Nurr1 as a transrepressor of NF-κB-regulated genes in glia demonstrated that this receptor is a potential target for development of therapeutic agents for treatment of neuroinflammatory disease (Saijo et al., 2009). Our studies with the *para*-phenyl substituted diindolylmethane demonstrate that this compound induces anti-inflammatory activity in glial cells through a Nurr1-dependent mechanism. Pharmacological stimulation of Nurr1-mediated transrepression by C-DIM12 represents a novel mechanism to decrease expression of NF-κB-regulated inflammatory genes in glial cells relevant to neurodegenerative disease.

Molecular Pharmacology Fast Forward. Published on April 9, 2015 as DOI: 10.1124/mol.114.095398
This article has not been copyedited and formatted. The final version may differ from this version.

Authorship Contributions

Participated in research design: De Miranda, Popichak, Hammond, Safe, and Tjalkens.

Conducted experiments: De Miranda, Popichak, Hammond, Jorgensen, Phillips.

Contributed new reagents or analytic tools: Safe

Performed data analysis: De Miranda, Popichak, Hammond, Jorgensen, and Tjalkens

Wrote or contributed to the writing of the manuscript: De Miranda, Popichak, Hammond, Safe, and Tjalkens.

References

Bensinger, S.J., and (null) (2009). A Nurr1 pathway for neuroprotection. Cell *137*, 3.

Brambilla, R., Bracchi-Ricard, V., Hu, W.-H., Frydel, B., Bramwell, A., Karmally, S., Green, E.J., and Bethea, J.R. (2005). Inhibition of astroglial nuclear factor kappaB reduces inflammation and improves functional recovery after spinal cord injury. J. Exp. Med. *202*, 145–156.

Carbone, D.L., Popichak, K.A., Moreno, J.A., Safe, S., and Tjalkens, R.B. (2008). Suppression of 1-Methyl-4-phenyl-1,2,3,6-tetrahydropyridine-Induced Nitric-Oxide Synthase 2 Expression in Astrocytes by a Novel Diindolylmethane Analog Protects Striatal Neurons against Apoptosis. Molecular Pharmacology *75*, 35–43.

Cho, I.-H., Hong, J., Suh, E.C., Kim, J.H., Lee, H., Lee, J.E., Lee, S., Kim, C.-H., Kim, D.W., Jo, E.-K., et al. (2008). Role of microglial IKKbeta in kainic acid-induced hippocampal neuronal cell death. Brain *131*, 3019–3033.

Chu, Y., Le, W., Kompoliti, K., Jankovic, J., Mufson, E.J., and Kordower, J.H. (2006). Nurr1 in Parkinson's disease and related disorders. J. Comp. Neurol. *494*, 495–514.

Dae Cho, S., Lee, S.O., Chintharlapalli, S., Abdelrahim, M., Khan, S., Yoon, K., Kamat, A.M., and Safe, S. (2010). Activation of Nerve Growth Factor-Induced B by Methylene-Substituted Diindolylmethanes in Bladder Cancer Cells Induces Apoptosis and Inhibits Tumor Growth. Molecular Pharmacology *77*, 396–404.

De Miranda, B.R., Miller, J.A., Hansen, R.J., Lunghofer, P.J., Safe, S., Gustafson, D.L., Colagiovanni, D., and Tjalkens, R.B. (2013). Neuroprotective efficacy and pharmacokinetic behavior of novel anti-inflammatory para-phenyl substituted diindolylmethanes in a mouse

model of Parkinson's disease. Journal of Pharmacology and Experimental Therapeutics *345*, 125–138.

De Miranda, B.R., Popichak, K.A., Hammond, S.L., Miller, J.A., Safe, S., and Tjalkens, R.B. (2014). Novel Para-Phenyl Substituted Diindolylmethanes Protect Against MPTP Neurotoxicity and Suppress Glial Activation in a Mouse Model of Parkinson's Disease. Toxicological Sciences.

Debernard, K.B., and Mathisen, G.H. (2012). Differences in NGFI-B, Nurr1, and NOR-1 expression and nucleocytoplasmic translocation in glutamate-treated neurons. … International.

Fan, X., Luo, G., Ming, M., Pu, P., Li, L., Yang, D., and Le, W. (2009). Nurr1 expression and its modulation in microglia. Neuroimmunomodulation *16*, 162–170.

García-Yagüe, Á.J., Rada, P., Rojo, A.I., Lastres-Becker, I., and Cuadrado, A. (2013). Nuclear import and export signals control the subcellular localization of Nurr1 protein in response to oxidative stress. Journal of Biological Chemistry *288*, 5506–5517.

Ghosh, S., May, M.J., and Kopp, E.B. (1998). NF-kappa B and Rel proteins: evolutionarily conserved mediators of immune responses. Annu. Rev. Immunol. *16*, 225–260.

Gilmore, T.D. (2006). Introduction to NF-kappaB: players, pathways, perspectives. Oncogene *25*, 6680–6684.

Glass, C.K., Saijo, K., Winner, B., Marchetto, M.C., and Gage, F.H. (2010). Mechanisms Underlying Inflammation in Neurodegeneration. Cell *140*, 918–934.

He, B.P., Wen, W., and Strong, M.J. (2002). Activated microglia (BV-2) facilitation of TNF-alpha-mediated motor neuron death in vitro. J. Neuroimmunol. *128*, 31–38.

Inamoto, T., Papineni, S., Chintharlapalli, S., Cho, S.D., Safe, S., and Kamat, A.M. (2008). 1,1-Bis(3'-indolyl)-1-(p-chlorophenyl)methane activates the orphan nuclear receptor Nurr1 and inhibits bladder cancer growth. Molecular Cancer Therapeutics *7*, 3825–3833.

Kim, S.H., Smith, C.J., and Van Eldik, L.J. (2004). Importance of MAPK pathways for microglial pro-inflammatory cytokine IL-1 beta production. Neurobiology of Aging *25*, 431–439.

Krishnan, N., Bencze, G., Cohen, P., and Tonks, N.K. (2013). The anti-inflammatory compound BAY-11-7082 is a potent inhibitor of protein tyrosine phosphatases. Febs J. *280*, 2830–2841.

Lee, S.-O., Li, X., Hedrick, E., Jin, U.-H., Tjalkens, R.B., Backos, D.S., Li, L., Zhang, Y., Wu, Q., and Safe, S. (2014). Diindolylmethane Analogs Bind NR4A1 and Are NR4A1 Antagonists in Colon Cancer Cells. Mol. Endocrinol. me20141102.

Lee, S.-O., Li, X., Khan, S., and Safe, S. (2011). Targeting NR4A1 (TR3) in cancer cells and tumors. Expert Opin. Ther. Targets *15*, 195–206.

Li, X., Lee, S.-O., and Safe, S. (2012). Structure-dependent activation of NR4A2 (Nurr1) by 1,1-bis(3'-indolyl)-1-(aromatic)methane analogs in pancreatic cancer cells. Biochem. Pharmacol. *83*, 1445–1455.

Livak, K.J., and Schmittgen, T.D. (2001). Analysis of relative gene expression data using real-time quantitative PCR and the 2(-Delta Delta C(T)) Method. Methods *25*, 402–408.

Maguire-Zeiss, K.A., and Federoff, H.J. (2010). Future directions for immune modulation in neurodegenerative disorders: focus on Parkinson's disease. J Neural Transm *117*, 1019–1025.

Nolan, Y.M., Sullivan, A.M., and Toulouse, A. (2013). Parkinson's disease in the nuclear age of neuroinflammation. Trends Mol Med *19*, 187–196.

Polazzi, E., and Monti, B. (2010). Microglia and neuroprotection: from in vitro studies to therapeutic applications. Prog. Neurobiol. *92*, 293–315.

Qin, C., Morrow, D., Stewart, J., Spencer, K., Porter, W., Smith, R., Phillips, T., Abdelrahim, M., Samudio, I., and Safe, S. (2004). A new class of peroxisome proliferator-activated receptor gamma (PPARgamma) agonists that inhibit growth of breast cancer cells: 1,1-Bis(3'-indolyl)-1-(p-substituted phenyl)methanes. Molecular Cancer Therapeutics *3*, 247–260.

Saijo, K., Crotti, A., and Glass, C.K. (2013). Regulation of microglia activation and deactivation by nuclear receptors. Glia *61*, 104–111.

Saijo, K., Winner, B., Carson, C.T., Collier, J.G., Boyer, L., Rosenfeld, M.G., Gage, F.H., and Glass, C.K. (2009). A Nurr1/CoREST Pathway in Microglia and Astrocytes Protects Dopaminergic Neurons from Inflammation-Induced Death. Cell *137*, 47–59.

Saucedo-Cardenas, O., Quintana-Hau, J.D., Le, W.D., Smidt, M.P., Cox, J.J., De Mayo, F., Burbach, J.P., and Conneely, O.M. (1998). Nurr1 is essential for the induction of the dopaminergic phenotype and the survival of ventral mesencephalic late dopaminergic precursor neurons. Proc. Natl. Acad. Sci. U.S.a. *95*, 4013–4018.

Tansey, M.G., and Goldberg, M.S. (2010). Neuroinflammation in Parkinson's disease: Its role in neuronal death and implications for therapeutic intervention. Neurobiology of Disease *37*, 510–518.

Yoon, K., Lee, S.-O., Cho, S.D., Kim, K., Khan, S., and Safe, S. (2011). Activation of nuclear TR3 (NR4A1) by a diindolylmethane analog induces apoptosis and proapoptotic genes in pancreatic cancer cells and tumors. Carcinogenesis *32*, 836–842.

Zhang, T., Wang, P., Ren, H., Fan, J., and Wang, G. (2009). NGFI-B nuclear orphan receptor Nurr1 interacts with p53 and suppresses its transcriptional activity. Mol Cancer Res *7*, 1408–1415.

Zhao, Y., and Bruemmer, D. (2010). NR4A orphan nuclear receptors: transcriptional regulators of gene expression in metabolism and vascular biology. Arterioscler. Thromb. Vasc. Biol. *30*, 1535–1541.

Molecular Pharmacology Fast Forward. Published on April 9, 2015 as DOI: 10.1124/mol.114.095398
This article has not been copyedited and formatted. The final version may differ from this version.

Footnotes:

This work was supported by grants from the Michael J. Fox Foundation for Parkinson's Research and the Consolidated Anti-Aging Foundation, as well as grants from the National Institutes of Health [Grants ES021656, P30-023512].

b) Meeting abstracts- None

c) Please send reprint requests to:

Ronald B. Tjalkens

1680 Campus Delivery

Fort Collins, CO 80523

Ron.Tjalkens@colostate.edu

d) Authors: [1]Briana R. De Miranda, [2]Katriana A. Popichak, [3]Sean L. Hammond, [4]Bryce A. Jorgensen, [5]Aaron T. Philips, [6]Stephen Safe, [7]Ronald B. Tjalkens.

Molecular Pharmacology Fast Forward. Published on April 9, 2015 as DOI: 10.1124/mol.114.095398
This article has not been copyedited and formatted. The final version may differ from this version.

Figure Legends

Figure 1. C-DIM inflammatory gene suppression in glia is structure-dependent. Primary murine mixed glial cultures were treated with saline or 1 μg/ml LPS and 1 μM or 10 μM of DIM-C-pPhOCH3 (C-DIM5), DIM-C-pPhPh (C-DIM9), of DIM-C-pPhCl (C-DIM12) for 8 hours, and assessed for **A.** *Nos2* or **B.** *Il-1β* expression with real-time PCR. **C**. The structure of chloro-substituted C-DIM12. **D-I.** BV-2 microglia were treated with saline or 1 μg/ml LPS over a 24-hour time-point, and RNA was collected for real-time PCR analysis of cytokine mRNA expression. Data are expressed as mean ± SEM (n=4); mRNA fold change; internal control (β-actin). Statistical significance is expressed as mean compared to saline control; $^{*}(p < 0.05)$, $^{**}(p < 0.01)$, $^{****}(p < 0.0001)$.

Figure 2. Dose-dependent suppression of inflammatory genes in BV-2 microglia and NF-κB-transactivation in reporter cells. A-F. BV-2 microglia were pre-treated for 1 hour with 0.1 μM, 1.0 μM or 10 μM C-DIM12 followed by 24 hour LPS (1 μg/ml). mRNA expression was assessed for fold change of cytokine expression (β-actin internal control). Data are expressed as mean ± SEM (n=4); mRNA fold change. **G.** NF-κB/GFP/Luc HEK reporter cell line is induced by TNFα for GFP protein expression of NF-κB. **H.** Dose-response of NF-κB-GFP expression per cell (DAPI counterstain) in NF-κB/GFP/Luc HEK cells with increasing TNFα concentrations. **I.** NF-κB/GFP/Luc HEK cells were treated with C-DIM12 (25 μM, 50 μM, 100 μM) or Bay11 (30 μM, 50 μM) as a positive control for NF-κB suppression. **J.** Timecourse data from NF-κB/GFP/Luc HEK cells that received TNFα and were assayed over 24 hours with (gray line) or without (black line) 100 μM C-DIM12. mRNA assessed for fold change expression, data are expressed as mean ± SEM (n=16); $^{**}(p < 0.01)$, $^{***}(p < 0.001)$, $^{****}(p < 0.0001)$.

Molecular Pharmacology Fast Forward. Published on April 9, 2015 as DOI: 10.1124/mol.114.095398
This article has not been copyedited and formatted. The final version may differ from this version.

Figure 3. C-DIM12-dependent inhibition of inflammatory gene expression requires Nurr1. **A-C.** BV-2 microglia were treated with two different sequences of small interfering RNA (denoted RNAi-1, RNAi-2) or scrambled RNAi (Control RNAi). **D.** *NCor2, CoREST, HDAC3* mRNA was measured using real-time PCR following treatment with RNAi-1 (β-actin internal control). **E-F.** BV-2 microglia were treated with Nurr1-RNAi-1 or Control RNAi-1 for 24 hours followed by saline or 1 μg/ml LPS for 24 hours and assessed for mRNA expression of *Nos2* and *Tnfα*. **G-J.** BV-2 cells were treated with RNAi-1 or Control RNAi-1 for 24 hours followed by 10 μM C-DIM12 (1 hour pre-treatment) and 1 μg/ml LPS treatment and assessed for mRNA expression of *Nos2, Tnfα, Il-1β* and *Il-6*. Data are expressed as mean ± SEM (n=4); mRNA fold change. Statistical significance is compared to saline control; $^{*}(p < 0.05)$, $^{**}(p < 0.01)$, $^{***}(p < 0.001)$, $^{****}(p < 0.0001)$.

Figure 4. C-DIM12 does not prevent p65 translocation and blocks NF-κB-transactivation in reporter cells. **A.** BV-2 cells were treated with 10 μM C-DIM12 for one hour followed by saline or 1 μg/ml LPS for 30 min and fixed for immunofluorescence to examine p65 translocation; DAPI (blue), isolectin (green), p65 (red). **B**. p65 nuclear expression was quantified by mean fluorescence intensity encompassing the nuclei (DAPI boundary; background subtracted). **C.** Representative protein expression of phosphorylated p65 following LPS and LPS + C-DIM12 treatment. **D.** Relative optical density of phospho-p65 immunoblot, mean of three replicate experiments, protein levels were normalized to β-Actin (± SEM). **E-F.** BV-2 cells were treated with 30 μM SB216763 (SB21) to inhibit GSK3β for 1 hour, followed by 1 μg/ml LPS

Molecular Pharmacology Fast Forward. Published on April 9, 2015 as DOI: 10.1124/mol.114.095398
This article has not been copyedited and formatted. The final version may differ from this version.

and co-treatment with 10 μM C-DIM12 for 24 hours; data are expressed as mean ± SEM (n=3). $^{**}(p < 0.01)$, $^{***}(p < 0.001)$, $^{****}(p < 0.0001)$.

Figure 5. Nurr1 translocation and expression following LPS and C-DIM12 treatment. A-C. Primary mouse microglia were plated onto coverglass and treated with 10 μM C-DIM12 for one hour followed by 1 μg/ml LPS for 24 hours. Cells were fixed and imaged (100X) by confocal microscopy for immunofluorescence of Nurr1 (red), CD11b (green) and DAPI (blue). **D-E.** Quantification of Nurr1 protein translocation from the cytoplasm to the nucleus. **F.** *Nurr1* mRNA levels in BV-2 microglia treated with 1 μg/ml LPS, or 1 μg/ml LPS + 10 μM C-DIM12 for 24 hours. **G-H.** *Il-6* and *Nos2* mRNA levels from the same samples corresponding to Nurr1 mRNA. Data are expressed as mean ± SEM; mRNA fold change (n=3); $^{*}(p<0.05)$, $^{***}(p < 0.001)$, $^{****}(p < 0.0001)$. Scale bar = 10 μm.

Figure 6. C-DIM12 enhances Nurr1 recruitment to *Nos2* promoter, decreases p65 binding, and stabilizes binding of nuclear corepressors. BV-2 cells were treated with 10 μM C-DIM12 for one hour followed by 1 μg/ml LPS over a 24-hour time-point and assessed at the Nos2 promoter using chromatin immunoprecipitation (ChIP). **A.** The amount of p65 bound to the Nos2 promoter was measured in LPS or LPS + C-DIM treatments. **B.** The level of Nurr1 bound to the Nos2 promoter with or without C-DIM12 over a 24-hour timecourse with LPS. **C-D.** ChIP assessment of nuclear corepressor NCoR2 and corepressor complex CoREST bound to the Nos2 promoter. **E-F**. Representative protein quantitation of total Nurr1 and p65 following LPS and LPS + C-DIM12 treatment. **G.** NCoR2, HDAC3, and CoREST protein from 24 hour timecourse treatment with saline or LPS + 10 μM C-DIM12. **H-I**. Relative optical density of total cellular

Molecular Pharmacology Fast Forward. Published on April 9, 2015 as DOI: 10.1124/mol.114.095398
This article has not been copyedited and formatted. The final version may differ from this version.

corepressor protein expression, mean of three replicate experiments, protein levels were normalized to β-Actin (± SEM). **K.** Hypothesized mechanism by which C-DIM12 promotes Nurr1-dependent transrepression of p65 at the Nos2 promoter in BV-2 microglia. ChIP data are expressed as percent input ± SEM over control IgG (n=3);**($p < 0.01$), ***($p < 0.001$), ****($p < 0.0001$).

Molecular Pharmacology Fast Forward. Published on April 9, 2015 as DOI: 10.1124/mol.114.095398
This article has not been copyedited and formatted. The final version may differ from this version.

Table 1. Structure-dependent suppression of LPS-induced inflammation by C-DIMs

		Nos2 mRNA (Fold-Induction)		*Il-1β* mRNA (Fold-Induction)	
		Saline	**LPS**	**Saline**	**LPS**
		1 ± 0.2	240.5 ± 24.4*****	1.0 ± 0.2	175.7 ± 16.5*****
		LPS +		**LPS +**	
C-DIM	*R*-Group	**C-DIM (1 μM)**	**C-DIM (10 μM)**	**C-DIM (1 μM)**	**C-DIM (10 μM)**
1	-CF_3	160.6 ± 13.1	**50.8 ± 8.7**†	167.6 ± 18.2*****	**34.1 ± 3.1**†
2	-Br	175.5 ± 34.9	73.1 ± 23.1	129.4 ± 43.0	**40.6 ± 3.7**†
3	-F	133.8 ± 8.6	**3.3 ± 1.5**†	156.7 ± 10.6*****	**7.1 ± 1.8**†
4	-*tert*-Butyl	107.8 ± 20.5	84.8 ± 8.0	125.3 ± 8.0	93.9 ± 10.2
5	-OCH_3	141.4 ± 24.0	**14.7 ± 4.7**†	142.6 ± 6.1*****	**15.4 ± 2.3**†
6	-$N(CH_3)_2$	224.2 ± 68.0*****	99.5 ± 21.7	164.9 ± 30.0*****	65.1 ± 9.1
7	-H	184.9 ± 36.1*****	**12.4 ± 4.4**†	142.9 ± 44.5*****	**12.6 ± 2.3**†
8	-OH	189.3 ± 61.8*****	**0.7 ± 0.4**†	136.2 ± 48.3*****	**9.3 ± 1.4**†
9	-Phenyl	136.2 ± 47.7	180.9 ± 34.5*****	137.4 ± 47.4*****	127.2 ± 5.8
10	-CN	96.0 ± 21.6	**34.5 ± 5.8**†	140.1 ± 7.5*****	**23.8 ± 1.8**†
11	-CH_3	140.0 ± 5.5	**32.0 ± 6.8**†	152.2 ± 15.7*****	**36.4 ± 3.5**†
12	-Cl	180.4 ± 26.2	**60.6 ± 17.5**†	186.9 ± 27.6*****	**45.9 ± 8.9**†
13	-$COOCH_3$	255.5 ± 78.8*****	**90.9 ± 7.8**†	185.2 ± 11.5*****	**44.0 ± 15.2**†
14	-I	242.9 ± 83.9*****	**122.7 ± 33.5**†	161.4 ± 43.6*****	72.4 ± 15.0

*Different from Control group ($p < 0.05$)

Molecular Pharmacology Fast Forward. Published on April 9, 2015 as DOI: 10.1124/mol.114.095398
This article has not been copyedited and formatted. The final version may differ from this version.

[†]Different from LPS group ($p < 0.05$)

Table 1. Primary murine mixed glial cultures were treated with saline or 1 μg/ml LPS and 1 μM or 10 μM doses of one of 14 C-DIM analogs. Structural differences displayed as '*R*-Group' and significant suppression of *Nos2* and *Il-1β* mRNA levels from LPS control are indicated in bold. Data are expressed as mean ± SD, mRNA fold induction over LPS (β-actin internal control).

Figure 1

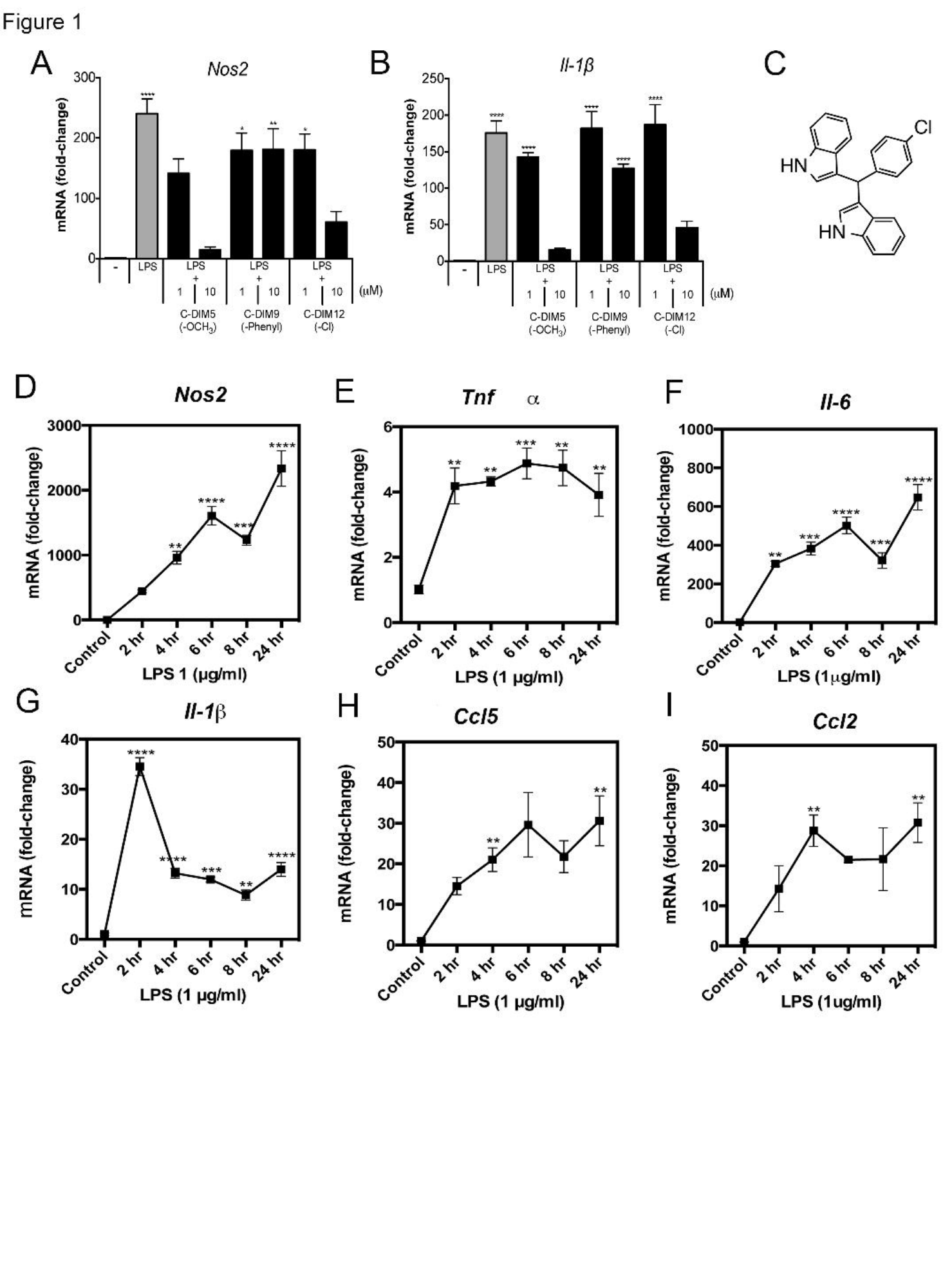
A
Nos2
mRNA (fold-change)
300
200
100
0
-
LPS
LPS + 1 | 10 (μM)
C-DIM5 (-OCH3)
C-DIM9 (-Phenyl)
C-DIM12 (-Cl)
B
Il-1β
mRNA (fold-change)
250
200
150
100
50
0
C
HN
HN
Cl
D
Nos2
mRNA (fold-change)
3000
2000
1000
0
Control
2 hr
4 hr
6 hr
8 hr
24 hr
LPS 1 (μg/ml)
E
Tnf α
mRNA (fold-change)
6
4
2
0
LPS (1 μg/ml)
F
Il-6
mRNA (fold-change)
1000
800
600
400
200
0
LPS (1μg/ml)
G
Il-1β
mRNA (fold-change)
40
30
20
10
0
LPS (1 μg/ml)
H
Ccl5
mRNA (fold-change)
50
40
30
20
10
0
LPS (1 μg/ml)
I
Ccl2
mRNA (fold-change)
50
40
30
20
10
0
LPS (1ug/ml)

Figure 2

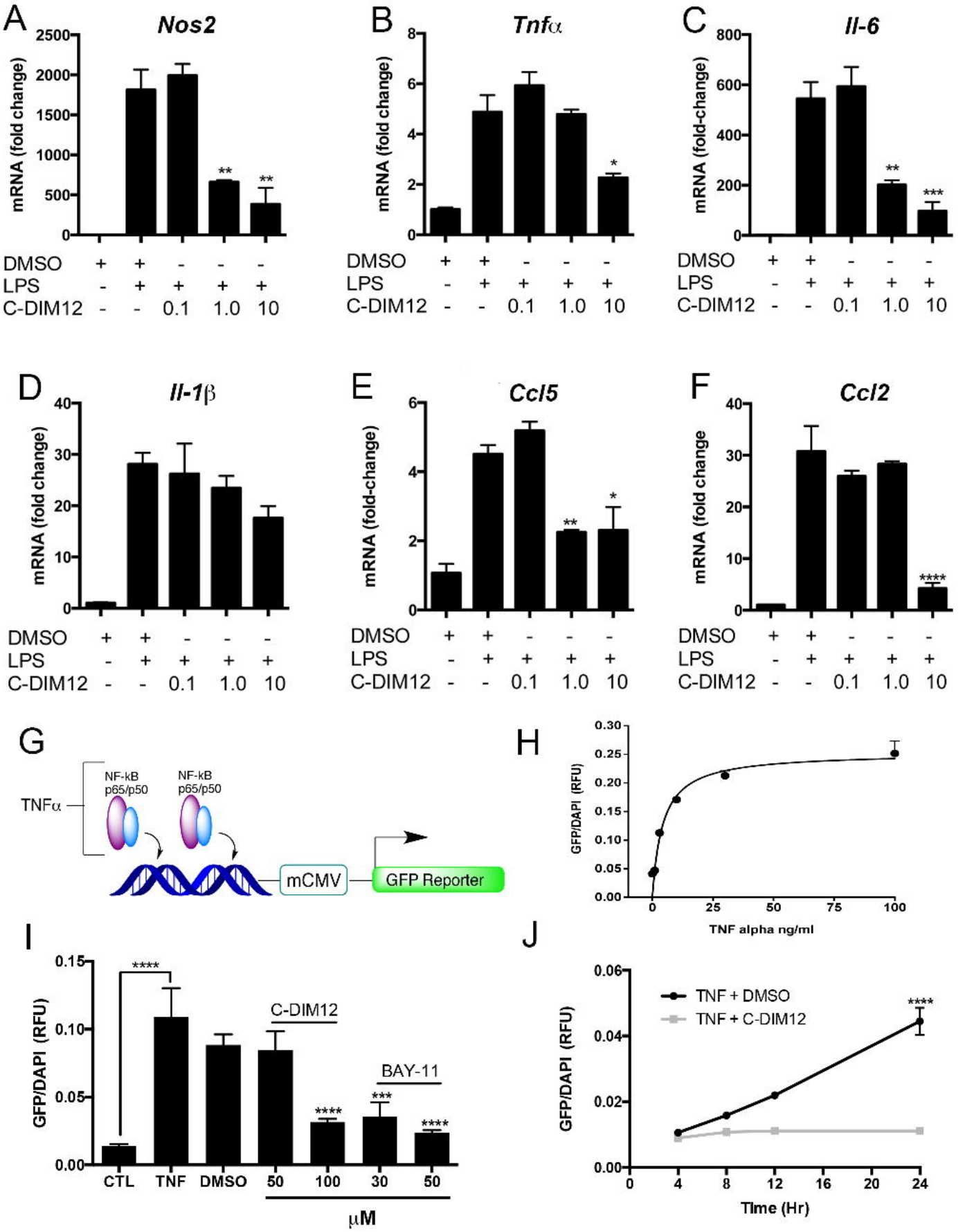
A
Nos2
mRNA (fold change)
2500
2000
1500
1000
500
0
**
**
DMSO + + - - -
LPS - + + + +
C-DIM12 - - 0.1 1.0 10
B
Tnfα
mRNA (fold change)
8
6
4
2
0
*
DMSO + + - - -
LPS - + + + +
C-DIM12 - - 0.1 1.0 10
C
Il-6
mRNA (fold-change)
800
600
400
200
0
**
***
DMSO + + - - -
LPS - + + + +
C-DIM12 - - 0.1 1.0 10
D
Il-1β
mRNA (fold change)
40
30
20
10
0
DMSO + + - - -
LPS - + + + +
C-DIM12 - - 0.1 1.0 10
E
Ccl5
mRNA (fold-change)
6
4
2
0
**
*
DMSO + + - - -
LPS - + + + +
C-DIM12 - - 0.1 1.0 10
F
Ccl2
mRNA (fold change
40
30
20
10
0
****
DMSO + + - - -
LPS - + + + +
C-DIM12 - - 0.1 1.0 10
G
TNFα
NF-kB p65/p50
NF-kB p65/p50
mCMV
GFP Reporter
H
GFP/DAPI (RFU)
0.30
0.25
0.20
0.15
0.10
0.05
0.00
0
25
50
75
100
TNF alpha ng/ml
I
GFP/DAPI (RFU)
0.15
0.10
0.05
0.00
****
C-DIM12
BAY-11
***
****
****
CTL
TNF
DMSO
50
100
30
50
μM
J
GFP/DAPI (RFU)
0.06
0.04
0.02
0.00
TNF + DMSO
TNF + C-DIM12
****
0
4
8
12
16
20
24
Time (Hr)

Figure 3

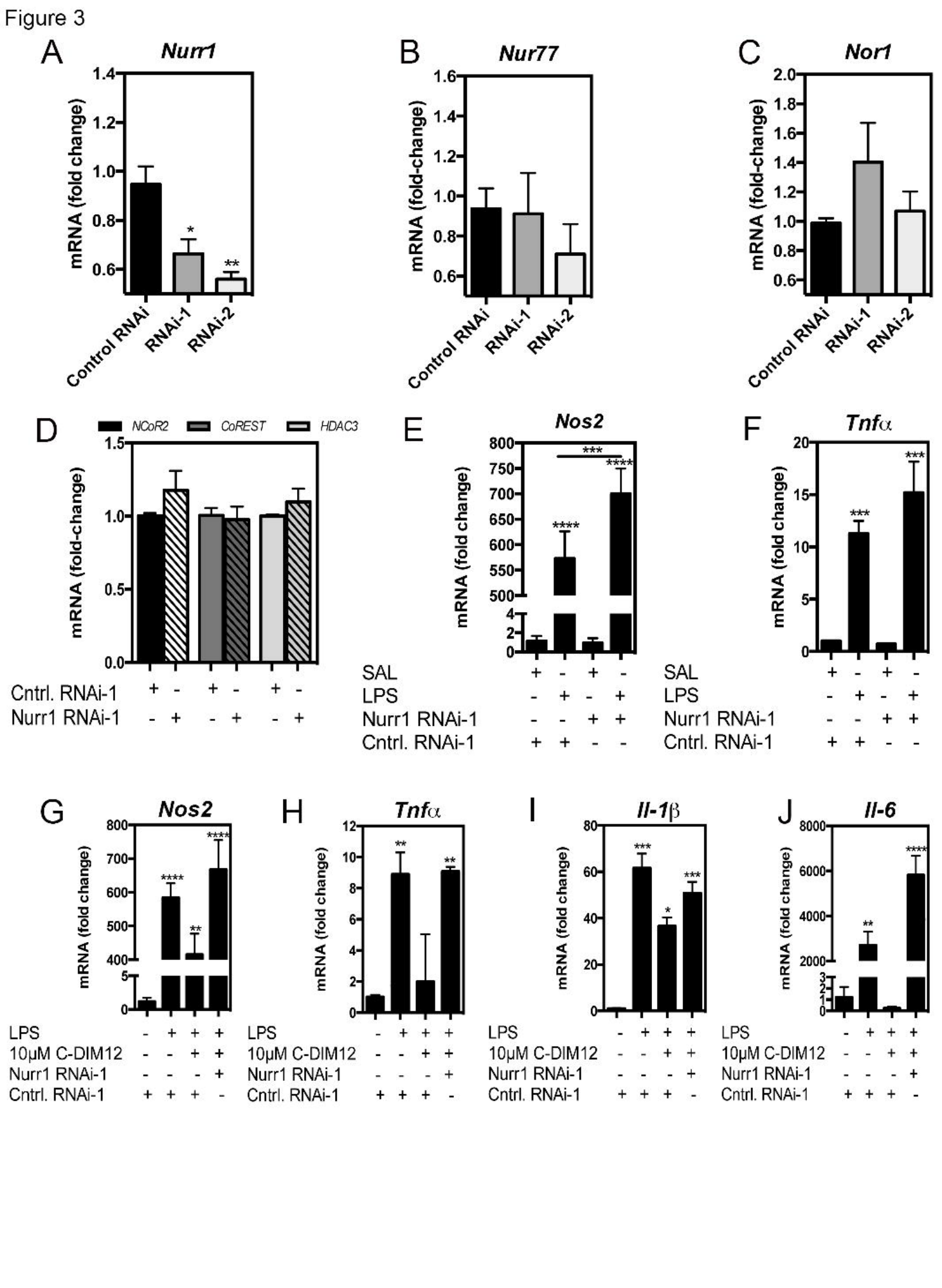
A
Nurr1
mRNA (fold change)
Control RNAi
RNAi-1
RNAi-2
B
Nur77
mRNA (fold-change)
C
Nor1
D
NCoR2
CoREST
HDAC3
Cntrl. RNAi-1
Nurr1 RNAi-1
E
Nos2
SAL
LPS
F
Tnfα
G
H
I
Il-1β
J
Il-6
10μM C-DIM12

Figure 4

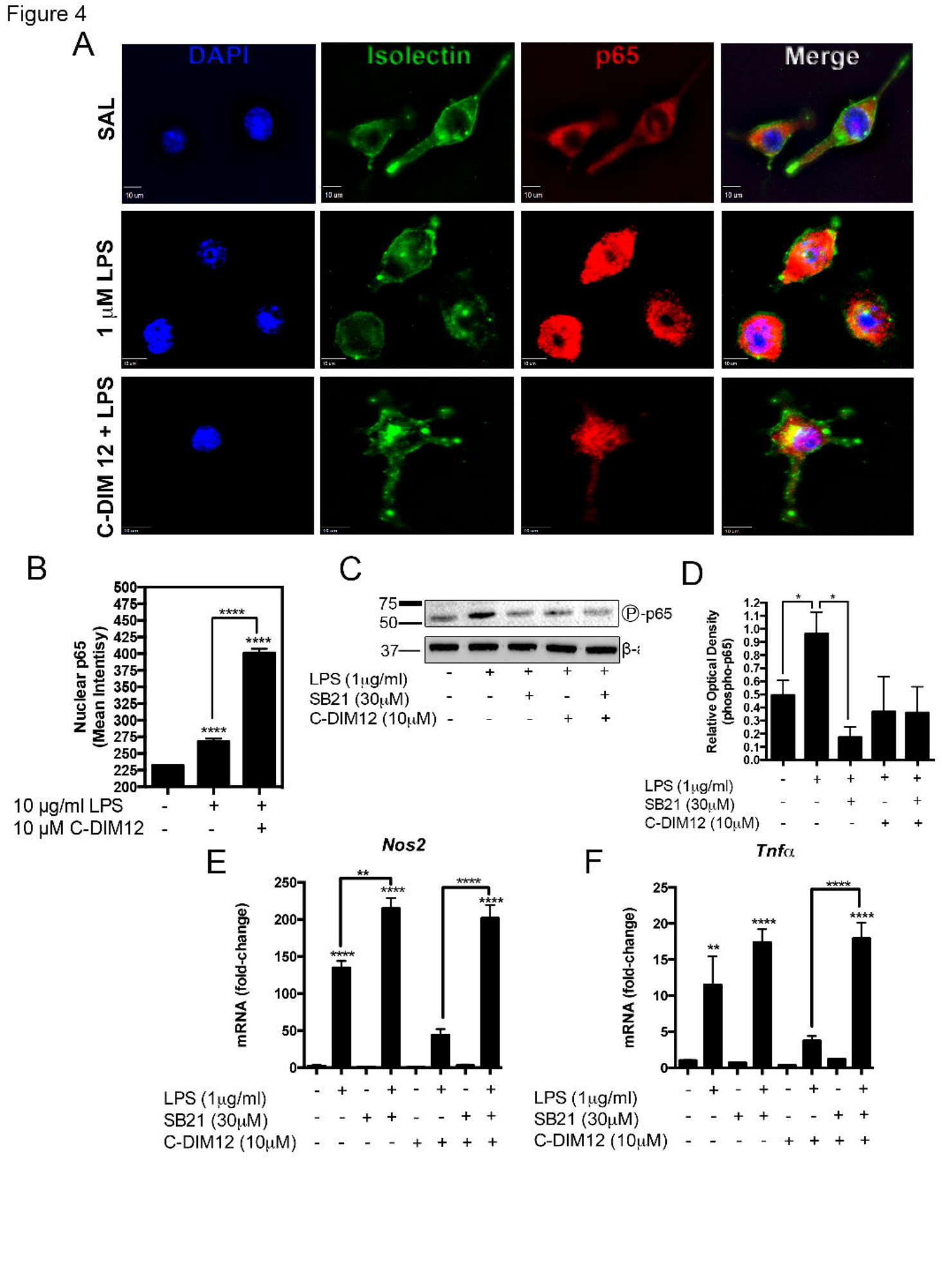
A
DAPI
Isolectin
p65
Merge
SAL
1 μM LPS
C-DIM 12 + LPS
B
Nuclear p65 (Mean Intentisy)
10 μg/ml LPS
10 μM C-DIM12
C
75
50
37
Ⓟ-p65
β-
LPS (1μg/ml)
SB21 (30μM)
C-DIM12 (10μM)
D
Relative Optical Density (phospho-p65)
LPS (1μg/ml)
SB21 (30μM)
C-DIM12 (10μM)
E
Nos2
mRNA (fold-change)
LPS (1μg/ml)
SB21 (30μM)
C-DIM12 (10μM)
F
Tnfα
mRNA (fold-change)
LPS (1μg/ml)
SB21 (30μM)
C-DIM12 (10μM)

Figure 5

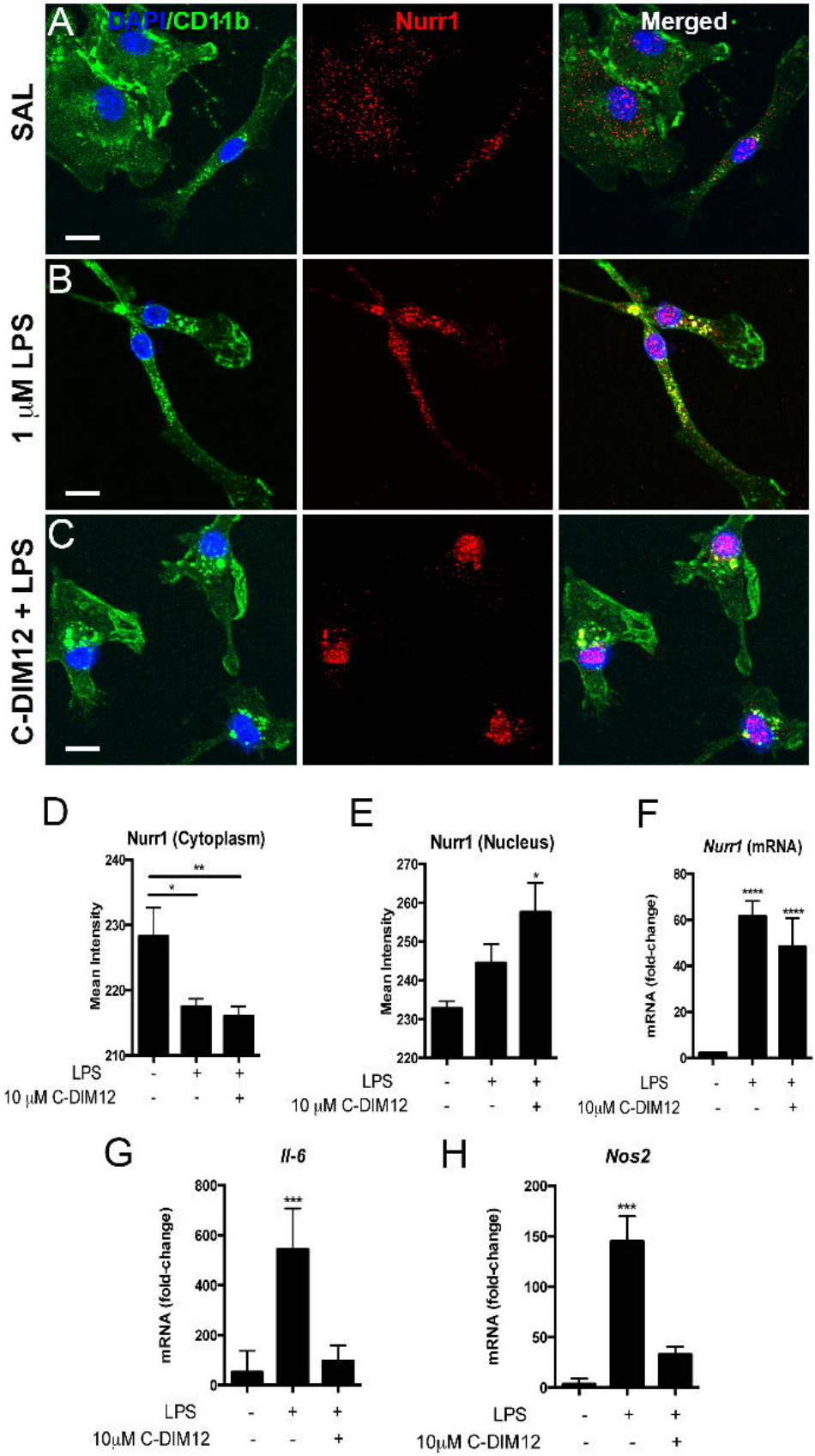
A
DAPI/CD11b
Nurr1
Merged
SAL
B
1 μM LPS
C
C-DIM12 + LPS
D
Nurr1 (Cytoplasm)
Mean Intensity
240
230
220
210
**
*
LPS - + +
10 μM C-DIM12 - - +
E
Nurr1 (Nucleus)
Mean Intensity
270
260
250
240
230
220
*
LPS - + +
10 μM C-DIM12 - - +
F
Nurr1 (mRNA)
mRNA (fold-change)
80
60
40
20
0
****
****
LPS - + +
10μM C-DIM12 - - +
G
Il-6
mRNA (fold-change)
800
600
400
200
0
***
LPS - + +
10μM C-DIM12 - - +
H
Nos2
mRNA (fold-change)
200
150
100
50
0
***
LPS - + +
10μM C-DIM12 - - +

Figure 6

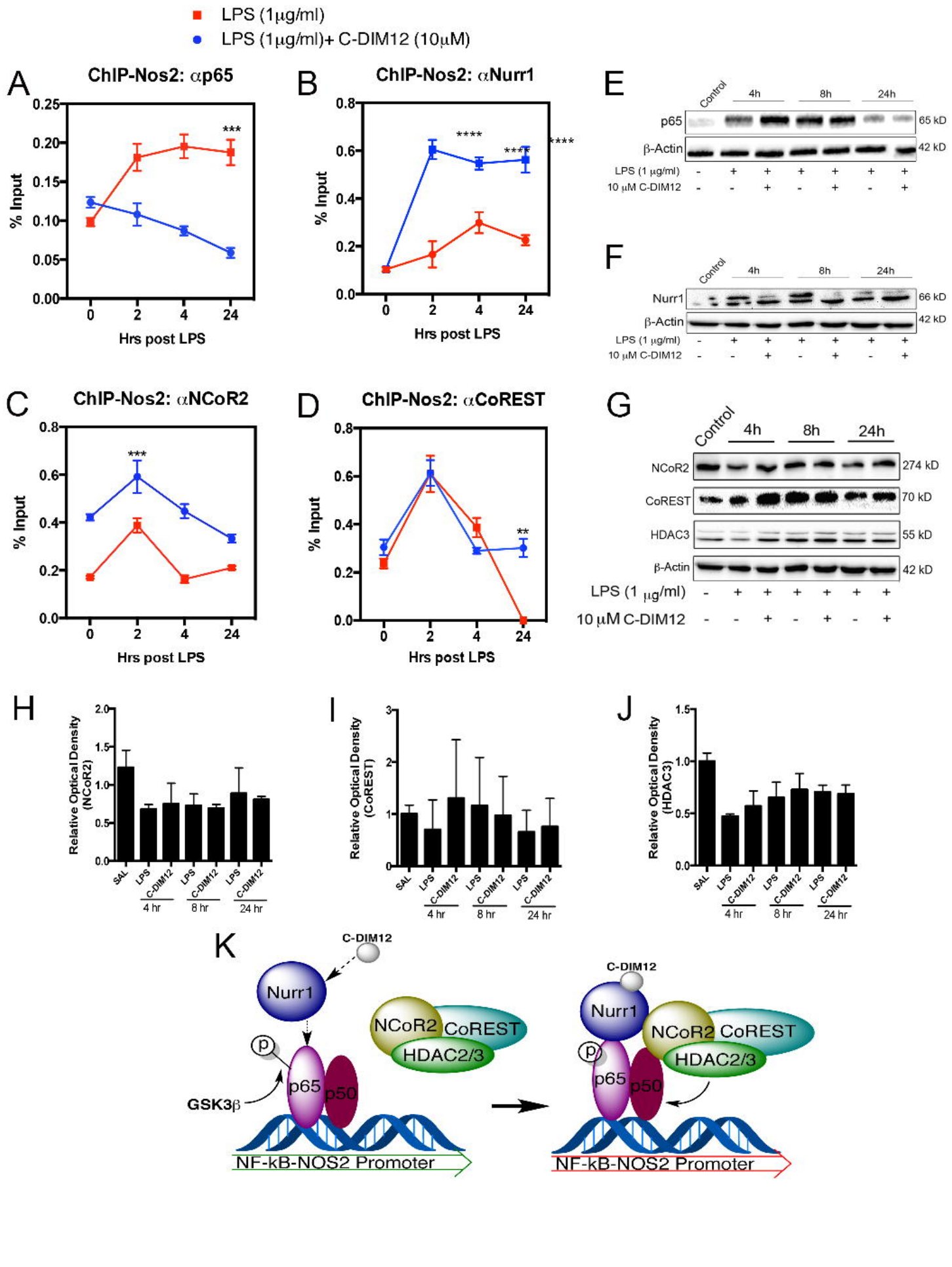
LPS (1μg/ml)
LPS (1μg/ml)+ C-DIM12 (10μM)
A
ChIP-Nos2: αp65
% Input
Hrs post LPS
B
ChIP-Nos2: αNurr1
% Input
Hrs post LPS
E
Control
4h
8h
24h
p65
65 kD
β-Actin
42 kD
LPS (1 μg/ml)
10 μM C-DIM12
F
Nurr1
66 kD
C
ChIP-Nos2: αNCoR2
D
ChIP-Nos2: αCoREST
G
NCoR2
274 kD
CoREST
70 kD
HDAC3
55 kD
H
Relative Optical Density (NCoR2)
I
Relative Optical Density (CoREST)
J
Relative Optical Density (HDAC3)
SAL
LPS
C-DIM12
4 hr
8 hr
24 hr
K
C-DIM12
Nurr1
NCoR2
CoREST
HDAC2/3
p
p65
p50
GSK3β
NF-kB-NOS2 Promoter